

Embrittlement and the Bistable Crystal Structure of Zirconium Hydride

G. J. Ackland

*Department of Physics and Astronomy, The University of Edinburgh,
Edinburgh, EH9 3JZ, Scotland, United Kingdom*

(Received 29 September 1997)

The stability of the ϵ phase of zirconium hydride is studied using the pseudopotential plane wave method. The fluorite structure is mechanically unstable with respect to a tetragonal distortion. However, the minimum corresponding to $c > a$ is almost degenerate in energy with that for $c < a$. The distortion explains the uniaxial misfit strain responsible for delayed hydride cracking in zirconium alloys. [S0031-9007(98)05482-9]

PACS numbers: 81.40.Np, 61.50.Ah, 62.20.Dc

Hydride formation can be a major factor in embrittlement of metallic components in a wide range of applications. In zirconium the mechanism involves, first, a migration of hydrogen to the strained region around the crack tip, causing local embrittlement and crack advance. This process is known as delayed hydride cracking (DHC) [1,2]. It can be modeled with continuum elasticity, but there is considerable dispute [3,4] as to the misfit strain of a hydride particle: although the overall unconstrained strain (the sum of the strains in all three directions) is known to be about 17%, assuming isotropic or uniaxial strain [5] gives rise to qualitatively different DHC models.

In titanium and zirconium alloys the stable hydride is the δ phase with a composition $M\text{H}_{2-x}$. Since the hydride typically has a larger lattice parameter than its host material, it can effectively be thought of as being under external strain and will grow preferentially in regions of tensile strain. To understand the effects of hydrides *in situ* one must therefore examine their behavior under strain. Examining nonhydrostatic strains is extremely difficult experimentally, but is tractable with *ab initio* computer simulations. In DHC both growth and elastic behaviors are important, so in this paper both crystal stability in the presence of an external strain and elastic response to changes in strain are addressed.

Zirconium dihydride ZrH_{2-x} is known to have a phase transition as a function of hydrogen concentration [6]. At $x = 0$ the crystal structure is face centered tetragonal (ϵ phase), but as x is increased, a transition to the cubic fluorite-type structure is observed (δ phase) [7]. In both of these phases, and in solid solution, the hydrogen is located in tetrahedral interstices between four zirconium atoms [8].

There is a well established model for the $\epsilon \rightarrow \delta$ transition as a function of hydrogen concentration: the reduced concentration allows hydrogen (vacancy) diffusion, equalizing the site occupancy and maximizing symmetry. What is not so obvious is why the stoichiometric compound should be noncubic, since across a wide range of compositions the hydrogen is located in the tetrahedral interstice as it would be in fluorite. Nor is it obvious why,

at an atomistic level, hydride formation should be such a dramatic embrittler [9].

This paper reports the results of *ab initio* pseudopotential calculations which have been carried out on the stoichiometric ZrH_2 compound to determine the strain dependence of the tetrahedral distortion. Calculations over a range of values for the c and a parameters allow the strain space around the fluorite structure to be mapped out. It is found that ZrH_2 has two possible distortions from cubic of extremely similar energy, separated by a barrier of order kT . This implies that there will be a dramatic softening of the C_{11} - C_{12} static tetragonal shear modulus with increased temperature, since a small applied stress will induce a transition between the two structures entailing a very large strain. Moreover, when precipitates form in an external strain field their distortion is extended along the direction of that strain, leading to uniaxial misfit strains which cause DHC.

We solve for the electronic charge density using a density functional framework [10] within the local density approximation to exchange and correlation [11,12] and repeated using the generalized gradient approximation [13]. Norm-conserving, nonlocal, Kleinman-Bylander pseudopotentials [14] generated using the Kerker method [15] are used. The electronic wave functions are expanded in a plane wave basis set up to a cutoff of 650 eV, which was found to converge total energy to within 0.01 eV per atom and the more important energy differences to 1%. The sampling of the Brillouin zone was done on a $5 \times 5 \times 5$ mesh which is reduced by symmetry to 18 special k points. This sampling was tested on the cubic hydride and was found to converge the total energy to 0.01 eV compared with meshes up to $10 \times 10 \times 10$, and converged energy differences to typically 0.001 eV or 5%. These calculations were carried out using established codes [16].

In view of the tiny difference in energy, close to the convergence criteria, the minimum energy structures found from the $5 \times 5 \times 5$ calculations were recalculated using a $10 \times 10 \times 10$ k -point set and a 750 eV cutoff. The results were unaffected.

Since the major source of error in these calculations arises from the local density approximation, the study was repeated using a generalized gradient approximation (GGA) [13]. This gives a better description of exchange and correlation in situations where there are large gradients in the electronic charge density such as free atoms, molecules, and surfaces. The improvement in the free atom leads to a better description of the cohesive energy of solids. In comparing bulk phases, the GGA has not offered a consistent improvement on the local-density approximation (LDA): both work well across a wide range of applications. In this case, where the energy differences are so small, comparing LDA and GGA will give some indication of the error associated with these approximations.

A number of tetragonal structures with varying c/a ratios were examined using LDA, and a contour plot of energy against the c and a parameter is shown in Fig. 1. Remarkably, the two minima corresponding to $c > a$ and $c < a$ were found to be within 0.004 eV per atom—smaller than the accuracy of these calculations and far below the thermal energy $k_b T$ at room temperature.

A similar plot for GGA is shown in Fig. 2. Apart from a rigid shift of about 0.5 eV, the two graphs are extremely similar. Once again the minimum corresponding to $c > a$ is slightly deeper—at 0.006 eV per atom.

In a further test of stability, a small orthorhombic distortion was applied to the minimum energy tetragonal structures. In each case this had the effect of increasing the energy, showing that the “freezing in” of the tetragonal instability along one (001) direction had the effect of stabilizing the instability in the (010) and (001) directions. Likewise, small displacements of the atoms confirmed the local stability of the tetragonal structure.

Ab initio calculations have proved themselves to be extremely reliable in evaluating minimum energy structures of various materials. We thus conclude that the two

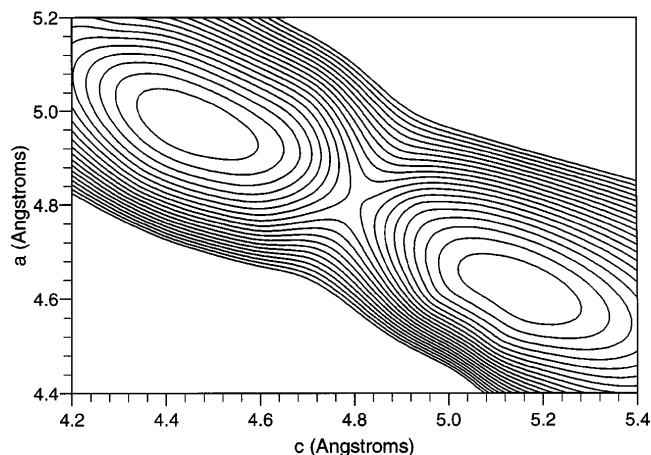


FIG. 1. Contour plot of energy against c and a for LDA calculations. The graph is produced by minimum curvature interpolation based on 50 data points. The contour interval is 0.01 eV and the graphs are truncated outside the central valley 0.2 eV above the minimum.

structures are almost degenerate, and any small nonhydrostatic stress could induce a transformation between them. The lattice parameters calculated for the $c < a$ structure (GGA: $c = 4.45$ Å, $a = 5.0$ Å; LDA: $c = 4.44$ Å, $a = 4.86$ Å) agreed extremely well with the experimental measured values ($c = 4.45$ Å, $a = 4.98$ Å), but it is curious that the $c > a$ structure (GGA: $c = 5.2$ Å, $a = 4.64$ Å; LDA: $c = 5.16$ Å, $a = 4.61$ Å) is predicted to be slightly more stable. It is possible that thermal effects could be the cause of this—the calculations are performed at zero temperature—or the fact that the hydride is prepared under modest pressure.

To attempt to determine the mechanism responsible for the instability, the density of electronic states has been calculated in the two minima and at the lowest energy cubic structure (see Fig. 3). These densities of states were taken from sampling over 1000 points in the Brillouin zone. All three structures have distinct band gaps of approximately 1 eV, and the only noticeable difference is an increase in the DOS of the lowest energy states. It is thus clear that the hydride is an insulating material and the distortion is not driven by any simple feature of the density of states such as an opening of the band gap.

The existence of two possible structures of ϵ zirconium hydride suggests the possibility of unusual responses to applied stresses. Figure 4 shows the stress-strain relationship for tetrahedral stress. Remarkably, this graph is almost discontinuous at the cubic structure. The reason for this is that even for a cubically symmetric ionic arrangement, the electronic structure is unstable against a tetragonal distortion.

Tetragonal symmetry was enforced on the charge density for all calculations used to produce the graphs above. The energy of the cubic structure was also calculated with the constraint of full cubic symmetry in the charge density and found to be significantly higher. The implication of this is that the Kohn-Sham [10] equation for the fluorite structure of ZrH_2 has three

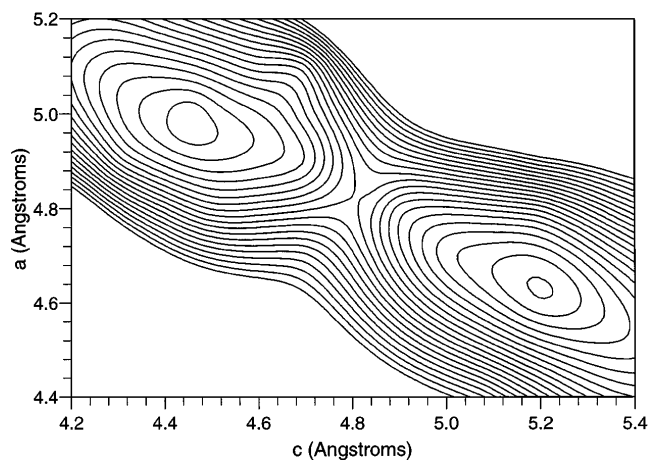


FIG. 2. Contour plot of energy against c and a for GGA calculations. The contour interval and truncations are identical to Fig. 1.

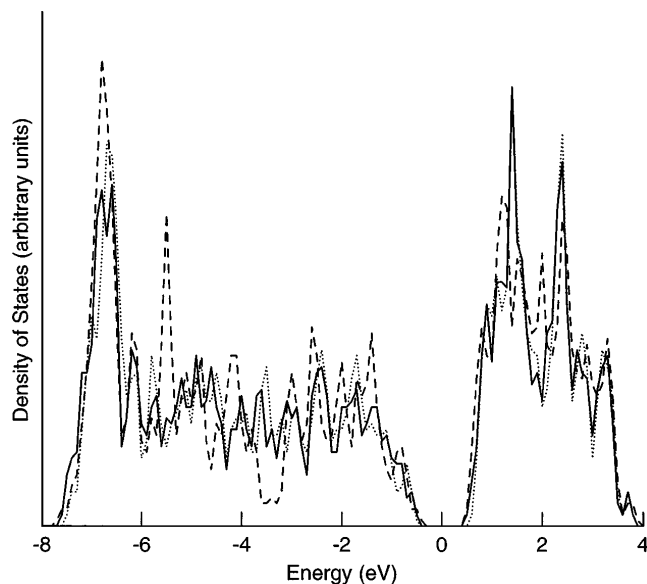


FIG. 3. Electronic density of states for cubic ZrH₂ (solid line) and the two minimum energy tetragonal ZrH₂ (dotted line: $c < a$; dashed line: $c > a$). The band gap is unaffected by the distortion, the major effect of the distortion being a shift of electrons into the lowest energy peak around -7 eV with predominantly s -type character.

different (symmetry-related) solutions, with the electronic structure spontaneously breaking the cubic symmetry of the ionic potential.

A small external tetragonal shear stress would tip the equilibrium structure from $c > a$ to $c < a$, the ensuing

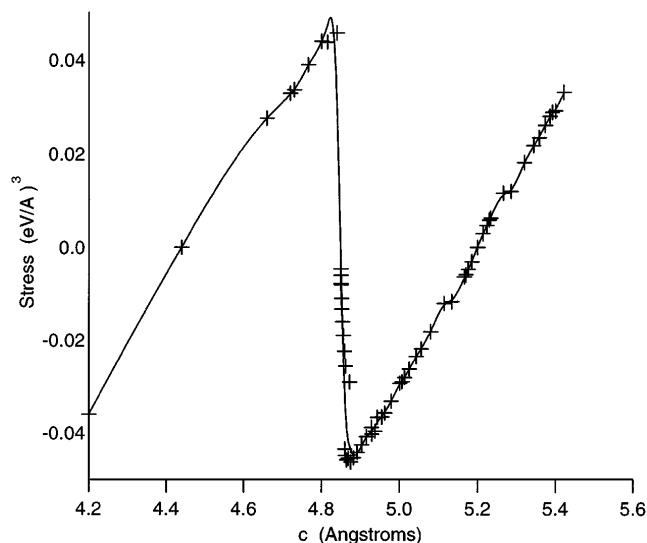


FIG. 4. Graph of σ_{zz} component of tetragonal stress [17] against c parameter taken from GGA calculations. At each point the value for a is chosen to be that for which $\sigma_{zz} = -2\sigma_{xx}$ so that the line represents pure tetragonal stress. It is found that the strain away from the nearest minimum or saddle point at each point along this line is very close to being purely tetragonal. Note the negative slope showing local instability at the cubic structure. The equivalent plot from LDA is extremely similar.

phase transformation being equivalent to a strain of around 13%. From the present calculations the tetragonal stress ($\sigma_{xx} = \sigma_{yy} = -\sigma_{zz}/2$) leading to a mechanical instability in the crystal is found from the peak values of Fig. 4 to be $\sigma_{xx} \approx 0.018$ eV/Å³ (250 N/mm²). However, at finite temperature the tetragonal strain may induce a transition to the lower energy structure since fluctuations will allow the barrier to be crossed. In this case the tetragonal stress required for the transition can be found from the common tangent between the two minima, and the transition stress can be calculated to be $\sigma_{xx} \approx 0.0015$ eV/Å³ (25 N/mm²), well below the yield stress. These tetragonal elastic stress-strain relations are shown in Fig. 4.

In a real crystal, hydride growth is constrained by the surrounding matrix, and will occur preferentially in regions of tensile strain. Because of the large miscibility gap [6], at equilibrium a precipitate of the cubic δ -phase will initially be formed. Being cubic, this has a 5% isotropic misfit strain.

As the hydrogen concentration increases by diffusion, the δ inclusion will become unstable: the stoichiometric δ -phase places the hydride on the negatively sloping central region of the stress-strain curve—an unstable equilibrium from which any tetragonal strain occurring will enhance the stress causing it.

The precipitate structure therefore transforms to the $c > a$ structure which is stabilized by, and oriented along the direction of, the uniaxial tensile strain ahead of the crack. The δ - ϵ phase transition has the effect of changing the hydride misfit strain from isotropic to uniaxial.

In DHC the hydride has been observed to grow in a lenticular shape in the plane of the crack. Since there is a uniaxial tensile region ahead of the crack tip, the tetragonally distorted structure will occur with its long axis normal to this plane. The 17% misfit strain is then oriented entirely normal to the plane, as required by the continuum models [2,4,5], and the hydrogen in the crack plane can migrate unhindered to the inclusion (hence the observed lenticular shape).

Once the crack enters the hydride, the region behind the crack tip will no longer be under tensile strain, and could transform to the $c < a$ phase, the boundary between regions of the two tetragonal phases being adjacent to the crack tip. Thus the bistable nature of the hydride could contribute directly to its embrittling effect.

In sum, it has been shown that cubic, stoichiometric ZrH₂ is unstable with respect to any tetragonal distortion, and that when grown ahead of a crack in a zirconium alloy, the stable crystal structure and its orientation is determined by the strain field giving rise to anisotropic misfit strains. Furthermore, the cubic structure is unusual in exhibiting multiple minima in the Kohn-Sham energy functional. While the calculations presented here are only for zirconium, it is plausible that a similar mechanism could operate in other materials which have a symmetry breaking distortion as a function of hydride concentration.

-
- [1] R. Dutton, *Metall. Trans. A* **8**, 1553 (1977).
[2] E. Smith, *J. Mater. Sci.* **30**, 5910 (1995).
[3] S. Q. Shi, M. Liao, and M. P. Puls, *Model. Simul. Mater. Sci. Eng.* **2**, 1065 (1994).
[4] E. Smith, *J. Mater. Sci.* **32**, 1121 (1997).
[5] G. C. Weatherly, *Acta Metall.* **29**, 501 (1981).
[6] E. Zuzek, J. P. Abriata, A. San-Martin, and F. D. Manchester, *Bulletin of Alloy Phase Diagrams* (American Society for Metals, Metals Park, Ohio, 1990), Vol. 11, No. 4.
[7] S. S. Sidhu, N. S. Satyamurty, F. P. Campos, and D. D. Zaubers, *Neutron and X-ray Studies on Non-Stoichiometric Metal Hydrides*, in *Advances in Chemistry* (American Chemical Society, Washington, DC, 1963), Vol. 39, p. 87.
[8] R. Khodabakhsh and D. K. Ross, *J. Phys. F* **12**, 15 (1982).
[9] J. H. Huang and C. S. Ho, *Mater. Chem. Phys.* **38**, 138–145 (1994).
[10] W. Kohn and L. J. Sham, *Phys. Rev.* **140**, 1133A (1965).
[11] J. P. Perdew and A. Zunger, *Phys. Rev. B* **23**, 5048 (1981).
[12] D. M. Ceperley and B. J. Alder, *Phys. Rev. Lett.* **45**, 566 (1980).
[13] J. P. Perdew, J. A. Chevary, S. H. Vosko, K. A. Jackson, M. R. Pederson, D. J. Singh, and C. Fiolhais, *Phys. Rev. B* **46**, 6671 (1992).
[14] L. Kleinman and D. M. Bylander, *Phys. Rev. Lett.* **48**, 1425 (1982).
[15] G. P. Kerker, *J. Phys. C* **13**, L189 (1980).
[16] The CASTEP code, originally written by M. C. Payne, is marketed by Molecular Simulations, Inc.
[17] O. H. Nielsen and R. M. Martin, *Phys. Rev. Lett.* **50**, 697 (1983).